

1 **Glacier extent and climate in the Maritime Alps during the Younger Dryas**

2 Matteo Spagnolo¹, Adriano Ribolini²

3 ¹ School of Geosciences, University of Aberdeen (UK) (corresponding author: m.spagnolo@abdn.ac.uk)

4 ² Dipartimento di Scienze della Terra, Università di Pisa (Italy)

5

6 Keywords: Younger Dryas; glacier reconstruction; equilibrium line altitude; palaeoclimate;
7 cosmogenic dates; Maritime Alps

8

9 Abstract

10 This study focuses on an Egesen-stadial moraine located at 1906-1920 m asl in the NE Maritime Alps,
11 Europe. Three moraine boulders are dated, via cosmogenic isotope analyses, to $12,490 \pm 1120$, $12,260$
12 ± 1220 and $13,840 \pm 1240$ yr, an age compatible with the Younger Dryas cooling event. The
13 reconstructed glacier that deposited the moraine has an equilibrium line altitude of 2349 ± 5 m asl,
14 calculated with an Accumulation Area Balance Ratio of 1.6. The result is very similar to the equilibrium
15 line altitude of another reconstructed glacier that deposited a moraine also dated to Younger Dryas,
16 in the SW Maritime Alps. The similarity suggests comparable climatic conditions across the region
17 during the cooling event. The Younger Dryas palaeoprecipitation is 1549 ± 26 mm/yr, calculated using
18 the empirical law that links precipitation and temperature at a glacier equilibrium line altitude, with
19 palaeotemperatures obtained from nearby palynological and chironomids studies. The
20 palaeoprecipitation is similar to the present, thus indicating non-arid conditions during the Younger
21 Dryas. This is probably due to the Maritime Alps peculiar position, at the crossroads between air
22 masses from the Mediterranean and the North Atlantic, the latter displaced by the southward
23 migration of the polar front. The equilibrium line altitude interval defined by the two reconstructed
24 glaciers, is used to model the extent of another 66 potential Younger Dryas glaciers in the region. Each
25 modelled glacier is reconstructed by iteratively changing the position of its front until the
26 reconstructed glacier has an ELA that falls within the interval. The result, which is checked against
27 geomorphological evidence, shows that glaciers covered 83.74 km^2 during the Younger Dryas, with a
28 volume of 5.39 km^3 . All valley heads were occupied by ice, except for the Maddalena/Larche Pass
29 (1999 m asl), an ideal site for future archaeological, palaeoecological and palaeozoological studies.

30

31

32 1. Introduction

33 The Younger Dryas (YD) is the most recent time in our planet's history during which a cooling
34 of the order of some degrees affected a large portion of the Earth, triggered by several climatic
35 processes (Renssen et al., 2015). It occurred at the end of the last glacial period, between 12.9 and
36 11.7 kyr (e.g. Johnsen et al., 2001; Broecker et al, 2010). The critical assemblage of several sources has
37 suggested that the cooling magnitude of this event was of the order of $2-8^\circ \text{ C}$ in the Northern
38 Hemisphere (Shakun and Carlson, 2010), with variations likely controlled by local climatic factors. One

39 of the most evident effects of the YD cooling on the Earth's surface is the widespread advancement
40 of alpine glaciers and the deposition of moraines. The lack of post-YD cooling events of similar or larger
41 magnitude, means that YD moraines are usually well preserved, as they have not been destroyed or
42 remoulded by the overriding of later glacier advances. Indeed, moraines dated back to the YD can be
43 found in many alpine regions worldwide (Ehlers and Gibbard, 2004). The European Alps are one of the
44 first regions where YD moraines have been identified and dated. Here, moraines belonging to the
45 Alpine glacier advance (or chronology stadial) known as the Egesen stadial have been recognised and
46 studied for a long time (e.g. Heuberger, 1968; Patzelt, 1972). The age of the Egesen moraines has been
47 attributed to the YD, initially via morphotratigraphic reconstructions and, in recent decades, by means
48 of cosmogenic isotope nuclide dating techniques (e.g. Ivy-Ochs et al., 1996; 2009).

49 Frontal (terminal) moraines are the essential ingredient for the reconstruction of former
50 Alpine glaciers, as they indicate the furthest downvalley position (limit or margin) of the glacier.
51 Models can be applied to reconstruct the full extent of palaeo glaciers, given the location of a frontal
52 moraine and the present-day topography, assuming the latter has not undergone intense post-glacial
53 modifications (e.g. Benn and Hulton, 2010). The ice surface distribution per elevation (hypsometry) of
54 reconstructed glaciers can then be used to extract a palaeo Equilibrium Line Altitude (ELA), the
55 elevation on a glacier where ice ablation and accumulation are equal (Osmaston, 2005). Modern
56 glacier ELAs have been empirically demonstrated to relate to climate, precipitation and temperature
57 in particular (e.g. Ohmura et al., 1992). Thus, a palaeo ELA obtained from a glacier reconstruction
58 based on a dated glacial deposit can be used to infer the climatic conditions at the time of deposition
59 of the moraine (e.g. Hughes et al., 2007).

60 In order to fully analyse the palaeogeography of an alpine region and to quantify palaeo ice
61 extent and volume at a specific time, ideally all palaeoglaciers occupying the region at that time should
62 be reconstructed. Examples of region-wide glaciers reconstruction in alpine contexts exist, but are
63 usually limited to large ice caps and ice fields modelling exercises, more or less constrained by terrain
64 evidence (e.g. for the last glacial cycle in the Alps: Seguinot et al., 2018; for the LGM in the Alps:
65 Florineth and Schlüchter, 1998; Bini et al., 2009; Ehlers and Gibbard, 2004; for the YD in Scotland:
66 Gолledge et al., 2008; Boston et al., 2015). Regional model reconstructions are useful not only to gain
67 insight into the glaciological response to past climate changes but also to understand human activities
68 and behaviours (migrations, trading, land reclamation etc.) (e.g. Catto et al., 1996; Meyer et al., 2009;
69 Ravazzi et al., 2007; Serrano et al., 2015), as well as fauna and flora dynamics (e.g. extinctions, glacial
70 refugia, etc.) (e.g. Badino et al., 2018; Casazza et al., 2016; Garnier et al., 2004; Schönswetter et al.,
71 2005; Schorr et al., 2013; Stehlik, 2003). They also provide essential information to explain changes or

72 hiatuses in other palaeoclimate proxies, for example in alpine lake deposits and speleothems (e.g.
73 [Spotl and Mangini, 2007](#); [van der Bilt et al., 2018](#); [Isola et al., 2019](#)).

74 Here, we present an Egesen moraine in the Maritime Alps (southwestern-most European Alps)
75 dated to the YD by means of cosmogenic isotope analyses. We reconstruct the extent of the glacier
76 that deposited the moraine and we calculate its ELA. The result is combined with the ELA of another,
77 already reconstructed glacier, which deposited the YD-dated Pian del Praiet (PDP) moraine ([Federici
78 et al., 2008](#)), located some 40 km ESE, to define a regional YD ELA for the Maritime Alps. This is used
79 to extract the palaeoclimate conditions of the region at the YD and to reconstruct all potential YD
80 glaciers (66) in one of the main valley systems of this Alpine sector.

81

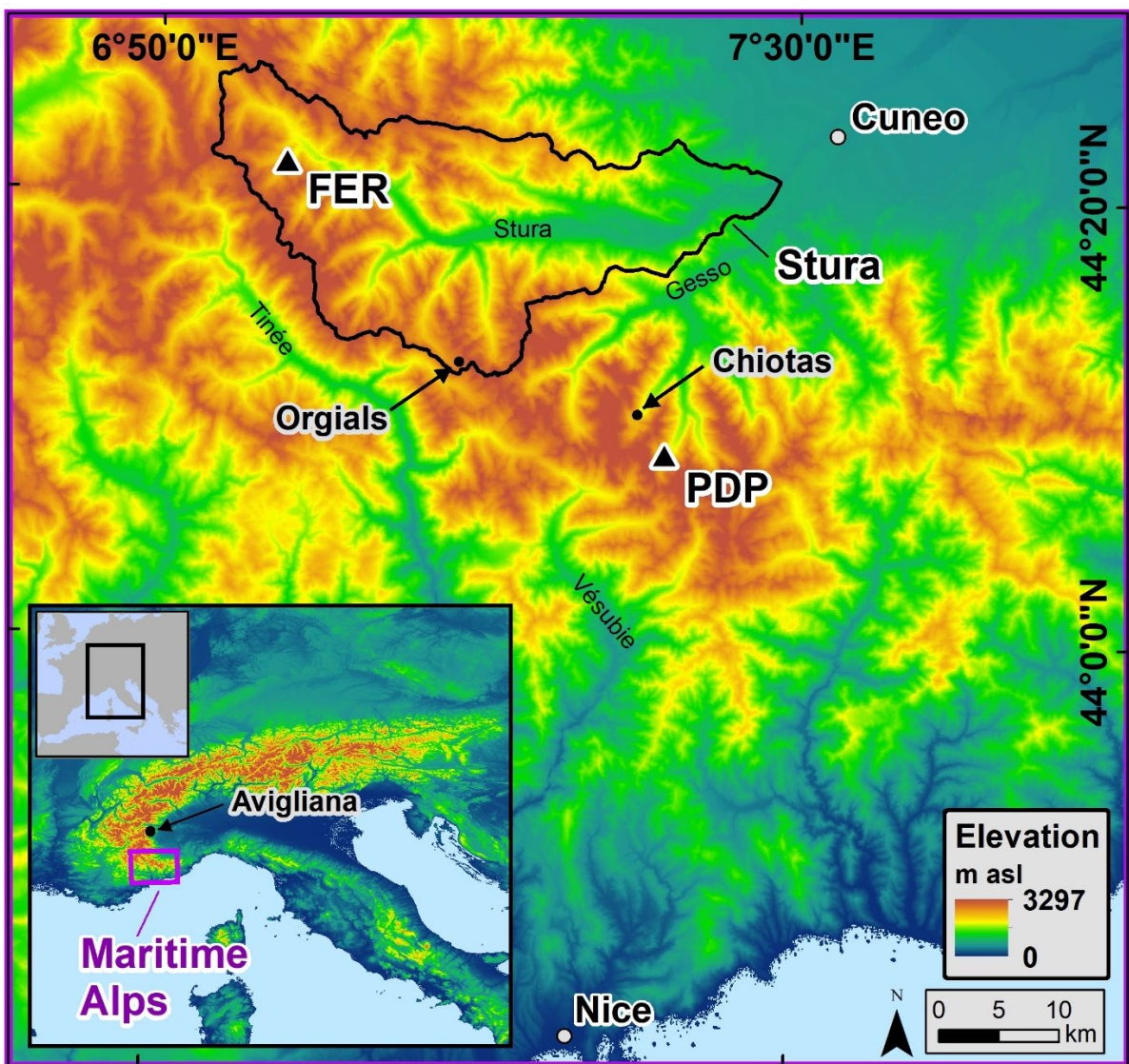
82

83 2. Regional context

84 The Maritime Alps are the southernmost (latitude of 43.9-44.4° N; longitude of 6.9-7.6° E)
85 portion of the European Alps, very close (40-60 km) to the Mediterranean Sea (hence the term
86 “Maritime”) and yet with elevations exceeding 3000 m asl (Figure 1). They are drained by four rivers,
87 which give name to the four main valleys of the region. These are the Tinée, Vesubié, Gesso and Stura
88 (di Demonte) rivers. The first two are located on the southwestern side of the Maritime Alps and drain
89 southward to the Ligurian Sea, while the last two, located on the northeastern side, ultimately drain
90 eastward, into the Po River and the Adriatic Sea. The Maritime Alps have been extensively glaciated
91 during Marine Isotope Stage 2, in line with the global Last Glacial Maximum (26-19 kyr) ([Clark et al.,
92 2009](#); [Shakun and Carlson, 2010](#); [Hughes et al., 2013](#)), when glaciers covered all main valleys and
93 extended towards, but did not reach, the Po Plain (Italy) to the north and the coast near Nice (France)
94 to the south ([Bigot-Cormier et al., 2005](#); [Federici et al., 2012](#)). While a number of moraines mapped in
95 the Maritime Alps have been hypothesised to belong to the Late Pleistocene ([Federici et al., 2003](#)),
96 only PDP moraine, located in the Gesso catchment, has so far been dated to the YD event (average
97 age of 13.2 ± 0.9 kyr) ([Federici et al., 2008](#); [2017](#)).

98 Present-day precipitations are bimodal, with peaks in spring and autumn, and are generally
99 lower than in the nearby northern Apennines and the rest of the Alps ([Isotta et al., 2014](#)).
100 Temperatures are unimodal with a summer peak, and generally higher than in other, nearby Alpine
101 regions ([Durand et al., 2009](#)). Differences exist across the main divide, with the southern side of the
102 Maritime Alps generally characterised by warmer temperatures than in the northern side ([Auer et al.,
103 2007](#)). However, within the studied region of interest, which lies entirely in the northern sector, similar
104 present-day climate conditions exist. This work focuses on the Stura catchment (Figure 1), one of the
105 largest in the southwestern Alps, comprising dozens of Alpine glacial valleys (currently ice-free),

106 covering an area of 615 km². The southern sector of the Stura catchment is generally characterised by
107 the crystalline rocks of the Argentera Massif, while its northern sector is made of sedimentary and
108 metasedimentary rock units (Malaroda et al., 1970). Tectonics has played a key control function on
109 the geometry development of these valleys (Ribolini, 2000; Musumeci et al., 2003, Ribolini and
110 Spagnolo, 2008). The dated moraine presented in this paper is in the Forneris Valley (Figure 1), in the
111 northern sector of the Stura catchment, at an elevation of 1908-1922 m asl. The upper valley, 3-3.5
112 km from the moraine, is characterised by peaks reaching >2700 m asl and comprises four glacial
113 cirques and a number of rock glaciers and glacial deposits. The specific lithology of the Forneris Valley
114 comprises high-grade schist, migmatite and quartzite rocks (Malaroda et al., 1970).
115



116
117 Figure 1. An overview of the Maritime Alps and the Stura catchment within it (outlined in black). The location of
118 the two moraines discussed in the text, PDP and FER (the latter in the Forneris Valley), is indicated, as well as
119 that of the chironomid site of Lago Piccolo di Avigliana ("Avigliana" in the figure), the pollen site of Laghi
120 dell'Orgials ("Orgials"), and the present-day weather station of the Diga del Chiotas ("Chiotas"). The cities of
121 Nice and Cuneo are shown to provide geographical references. The Mediterranean Sea is evidenced in light blue.

122

123 3. Methods

124 3.1 Chronology

125 The Ferrere (FER) moraine is located in the Forneris Valley, Stura catchment, near the village
126 of Ferrere (Figure 1). A total of 10 samples were collected from the moraine during two field
127 campaigns in 2011 and 2013. The <3-cm-thick samples were collected with hammer and chisel from
128 the upper, gently-sloping or horizontal, surface of large gneiss boulders located along the moraine
129 crest and emerging more than 1.5 m above the ground (Table 1 and Figure 2). Samples were crushed
130 and quartz grains extracted by using the standard ^{10}Be cosmogenic isotope analysis procedure (Kohl
131 and Nishizumi, 1992). Only 3 of the 10 samples revealed enough quartz of the right grain size for the
132 content of the isotope ^{10}Be to be measured. Measurements took place at the Natural Environment
133 Research Council - Cosmogenic Isotope Analysis Facility in the UK, with the use of the $2.79 \cdot 10^{-11}$
134 $^{10}\text{Be}/^9\text{Be}$ of Nishiizumi et al. (2007) for NIST 206 SRM4325 (NIST_27900 standardisation code,
135 equivalent to 07KNSTD). Reported exposure ages are calculated with the CRONUS-earth online
136 calculator version 2.3, using a default calibration data set and the time-independent Lal/Stone
137 spallation scheme.

138

139 3.2 Glacial reconstruction and ELA calculation

140 Glacier reconstructions in this paper are based on the application of a dedicated GIS tool,
141 “GlaRe” (Pellitero et al., 2016). The tool creates a 3D glacier surface based on the lateral interpolation
142 of a 2D glacier equilibrium profile, which is calculated by using a plastic rheology glacier model along
143 a user-defined flowline(s) (Benn and Hulton, 2010; Paterson, 1994, p.240; Shilling and Hollin, 1981).
144 Glaciers are reconstructed by extrapolating the ice thickness along the defined flowlines every 5 m,
145 and by applying a default shear stress of 100 kPa. Shape (F) factors (usually between 1 and 5),
146 accounting for the width of the glacial valley, are also included where appropriate, i.e. at different
147 points of valley narrowing. For each reconstructed glacier, the final GlaRe output is a 3D glacier terrain
148 model, which is obtained by interpolating sideways the ice thickness calculated along the flowlines,
149 using a “TOPOtoRASTER” interpolation approach (Pellitero et al., 2016). The reconstructed 3D glacier
150 terrain model is then used to extract the ELA of the glacier, through a separate GIS tool (Pellitero et
151 al., 2015). While the tool allows for most ELA calculation techniques to be implemented, for the sake
152 of consistency all our ELA calculations are based on the same technique, that of the Accumulation
153 Area Balance Ratio (AABR) (Furbish and Andrews, 1984), with an AABR value of 1.6, as recommended
154 for the Alps (Rea; 2009). AABR is considered one of the most robust techniques because it takes into
155 consideration both the hypsometry of the glacier surface (Osmaston, 2005) and the mass balance

156 gradients (Benn and Lehmkuhl, 2000). A contour interval of 10 m is set for the calculation of the glacier
157 surface area, meaning that all extrapolated ELA values have an associated calculation interval of ± 5
158 m (Pellitero et al., 2015).

159 A regional YD ELA interval is defined, based on the two ELAs values relative to glaciers that
160 deposited moraines dated to the YD (PDP and FER) in the Maritime Alps. The YD PDP moraine (Federici
161 et al., 2008) is located ~ 40 km to the SE of the FER moraine (Figure 1). The YD ELA interval is then used
162 to model the extent of all Stura catchment potential YD glaciers, which are largely located between
163 the two dated moraines (Figure 1). The modelled reconstruction is based on the application of the GIS
164 GlaRe and ELA tools (Pellitero et al., 2015, 2016) to all Stura glacial valleys. For each valley the tools
165 are run multiple times, iteratively moving up- or down-valley the hypothetical position of a glacier
166 front, until the reconstructed glacier returns an ELA value that fits within the defined regional YD ELA
167 interval. The approach is similar to that of Rea and Evans (2007) but is improved by the employment
168 of the GIS tools. The modelled position of the glaciers front was checked against evidence of frontal
169 moraines and glacial deposits from field observations, Quaternary information included in geological
170 maps (Malaroda et al., 1970) and remote sensing (Google Earth™).

171

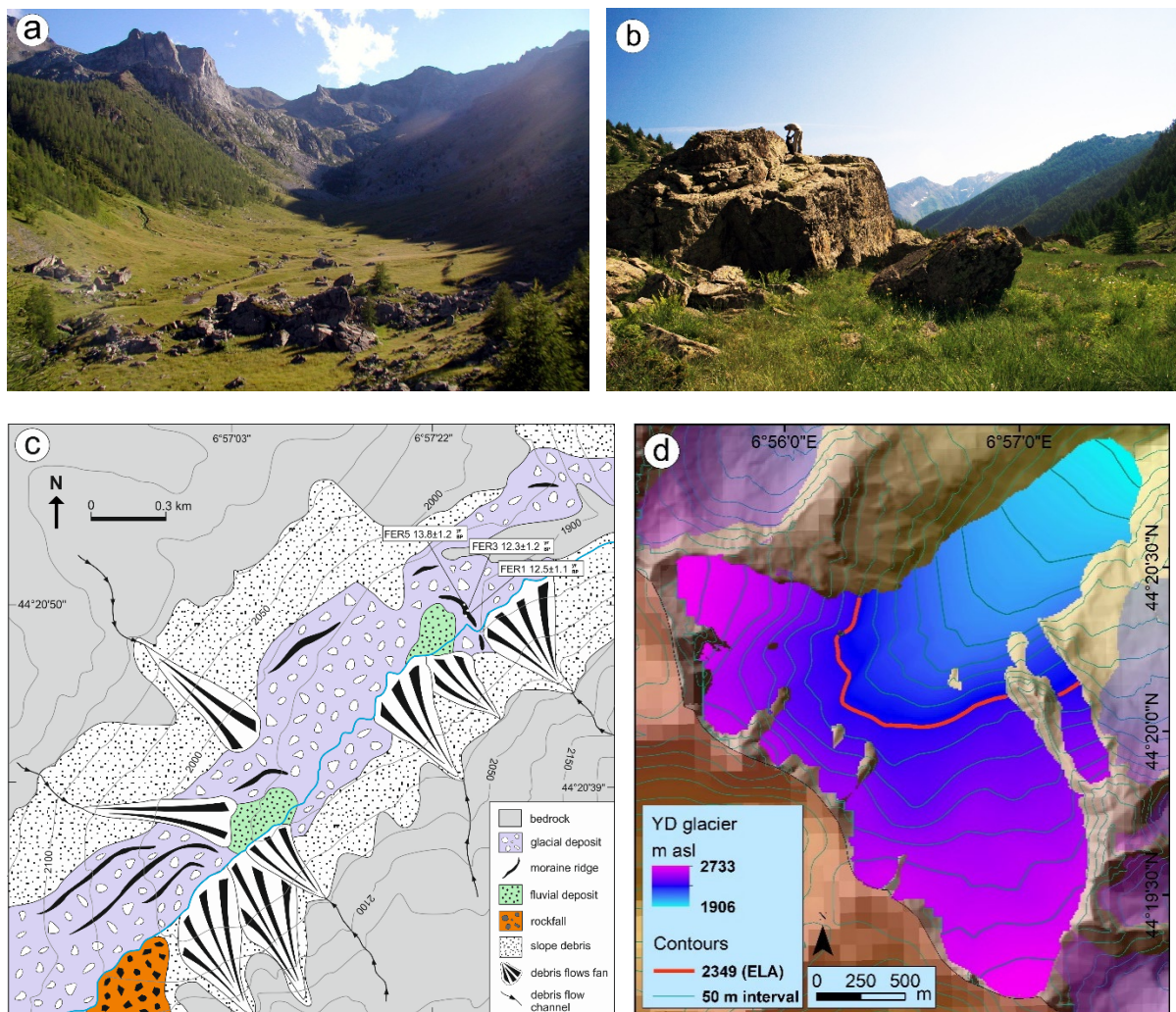
172 3.3 Palaeoclimatology

173 The climatological study is focused on the extraction of palaeoprecipitation at the YD ELA
174 (average of the two ELAs obtained from the reconstructed glaciers that deposited moraines dated
175 back to the YD in the Maritime Alps). This study is based on the empirical law connecting annual
176 precipitation (P_{ann} in mm) and mean air temperature during the melting period (the summer in our
177 case, T_{melt}) at the ELA, following the equation $P_{\text{ann}} = 5.87 T_{\text{melt}}^2 + 230 T_{\text{melt}} + 966$ (Ohmura and Boettcher,
178 2018). The temperature of the hottest month (T_{Jul}) for the YD in the region is sourced from
179 chironomids (midges), a fossil palaeotemperature proxy commonly found in freshwater lake deposits.
180 The chironomid series closest to the Maritime Alps and covering the YD period is found 95 km to the
181 north, at Lago Piccolo di Avigliana (45.0549°N, 7.3919°E; 365 m asl) (Larocque and Finsinger, 2008). At
182 this site, the average YD T_{Jul} is 16.3°C. In order to adjust this value to the elevation of the YD average
183 ELA we apply the present-day global lapse rate (6.5°C / 1km). While T_{Jul} is a good proxy for the
184 maximum monthly temperature and is very close to T_{melt} , for a precise calculation of the latter, T_{Jun}
185 and T_{Aug} also need to be taken into account and the temperature of the three months averaged. This
186 is achieved here by fitting a sine curve to the value of T_{Jul} and to the minimum monthly temperature
187 (T_{Jan}) (Brugger, 2006; Hughes and Braithwaite, 2008). The latter is obtained from a pollen study
188 conducted in one of the many lakes of the Stura catchment, the Orgials Lake, at 2240 m asl (Figure 1)
189 (Ortu et al., 2008). The average YD T_{Jan} for this site is -16.9°C, which is adjusted to the elevation of the

190 calculated YD ELA by using the standard lapse rate of 6.5°C / 1km. An attempt was also made to
 191 calculate T_{melt} with a different approach, based on a combination of the same chironomid data
 192 mentioned above and sea surface temperatures measured in northern Sicily (Cacho et al., 2001) and
 193 adjusted for the latitude and altitude of the ELA. However, the result is very similar to that obtained
 194 when combining chironomids with pollen data and, for the sake of clarity, we prefer to focus on the
 195 latter, which is based on proxies collected within or relatively close to the region of study.

196 In order to put the reconstructed YD palaeoclimate into context, we compare our calculation
 197 with present day measurements from a site within the Maritime Alps characterised by an elevation
 198 relatively close to the YD average ELA, namely the Diga del Chiotas weather station, which is at 1980
 199 m asl (Figure 1). Total annual precipitation, as well as January, July and summer (June-August)
 200 temperatures are averaged from 2001 to 2018 measurements. The measured temperatures are
 201 adjusted to the elevation of the calculated YD ELA by applying the standard lapse rate of 6.5°C / 1km.

202



203
204

205
206
207
208
209

Figure 2 An overview of the Ferrere moraine and of the Forneris glacier: (a) Val Forneris and Ferrere moraine in the foreground; (b) FER3 sampled boulder on the crest of the moraine (notice one of us over its top for scale); (c) geomorphological map of the Ferrere moraine and surroundings, with indication of the position of the three

210 dated boulder samples; (d) reconstructed YD Forneris glacier that deposited the Ferrere moraine and the
 211 calculated YD ELA (thick red line) obtained by using the AABR technique.

212
 213 4. Results

214 4.1 The Ferrere moraine and its age

215 FER is mainly composed of diamicton, with small (cms to dms) blocks immersed in abundant
 216 fine sediments. However, the most distinct trait of FER is the presence of a few, very large, angular
 217 blocks, with dimensions of up to 8 meters (Figure 2a, b). The blocks stand out of the ground and are
 218 aligned for about 350 m following a classic arcuate shape, typical of many marginal moraines. The
 219 frontal moraine deposit has clearly acted as a barrier to the natural flow of the main river, which now
 220 cuts the moraine into two halves. The relatively flat area right upvalley from the moraine is therefore
 221 characterised by a mixture of diamicton and fluvial sediments. The portion of other, less well
 222 preserved, lateral and frontal moraines exists in the immediate (~500 m) surroundings of FER (Figure
 223 2c), thus suggesting that multiple, most likely related to the same climatic event, glacier fluctuations
 224 (retreats and re-advances to a similar position) have occurred.

225 The Ferrere moraine samples, FER1, FER3 and FER5, returned ages of $12,490 \pm$ (external
 226 uncertainty, i.e. the sum of accelerator mass spectrometry measurement and production rate
 227 uncertainties) 1120 yr, $12,260 \pm 1220$ yr and $13,840 \pm 1240$ yr, respectively (Table 1). All three ages
 228 overlap in the 12,605-13,476 yr interval, with a weighted mean (\pm weighted standard deviation) of
 229 $12,950 \pm 700$ yr (calculated with iceTEA, Jones et al., 2019), and are therefore compatible with the YD
 230 timeframe. The FER ages are also similar to those of the other Maritime Alps moraine (PDP) dated
 231 back to the YD, which returned an average age of 13,174 yr (Federici et al., 2017).

232

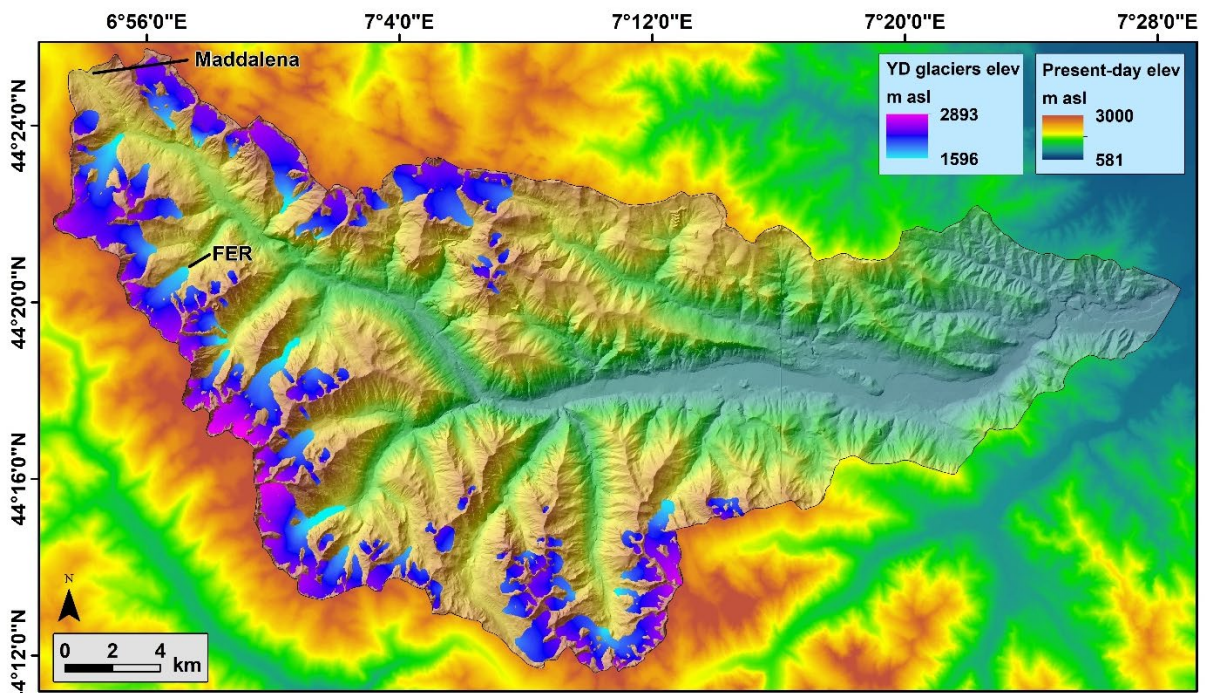
Sample name	rock type	Latitude (degree)	Longitude (degree)	boulder height (m)	strike (N)	dip (°)	Elevation (m asl)	Thickness (cm)	Density (g/cm ³)	Shielding factor	¹⁰ Be concentration (at/g)	¹⁰ Be uncertainty (at/g)	¹⁰ Be age yr BP	internal uncertainty (yr)	external uncertainty (yr)
FER1	gneiss	44.347136	6.957441	1.5-2.5	horiz.	flat	1908	<3	2.65	0.943	215,914	5,528	12,489	321	1117
FER3	gneiss	44.347302	6.957648	3-6	310	8 SW	1916	<3	2.65	0.942	213,360	10,774	12,257	621	1219
FER5	gneiss	44.347483	6.957622	2-5	70	20 SE	1915	<3	2.65	0.933	238,158	6,086	13,843	355	1238

233 Table 1 Detail of the three boulder samples from the moraine near the village of Ferrere, in Val Forneris,
 234 including their ¹⁰Be concentration and exposure age.
 235
 236

237 4.2 YD glaciers and ELA in the Maritime Alps

238 Identification of the Ferrere moraine, along with other glacial features, allowed for the
 239 reconstruction of the glacier responsible for its deposition, called here the Forneris glacier after the
 240 name of the valley. The reconstructed YD Forneris glacier (Figure 2d) has a length of 3.6 km from its
 241 margin (at ~1906 m asl) to a point close to the valley divide (at ~2733 m asl), covering an elevation
 242 range of 827 m. The glacier surface is 3.89 km² and its volume is 0.19 km³. The YD (AABR) ELA for the
 243 reconstructed Forneris glacier is 2349 ± 5 m asl. The ELA of the other Maritime Alps glacier with a
 244 moraine (PDP) dated to the YD, reconstructed with the same approach used here, is 2368 ± 5 m asl

245 (Federici et al., 2017). The two ELAs define a Maritime Alps YD ELA interval of 2344-2373 m asl, with
 246 an average value of 2358 ± 15 m asl. The extent of 66 other potential YD glaciers was modelled across
 247 the Stura catchment by iteratively changing their frontal position until their ELA fell within the 2344-
 248 2373 m asl interval (Figure 3 and Table 2). The area of the 66 glaciers ranges from 0.07 km² (Lake
 249 Sauma glacier) to 5.99 km² (Bernolfo glacier). Collectively, their area is 83.74 km² and the volume is
 250 5.39 km³, equivalent to 4.94 Gt of water.



251
 252 Figure 3 The 66 reconstructed YD glaciers in the Stura catchment of the Maritime Alps. “FER” indicates the
 253 position of the Ferrere moraine, while “Maddalena” (or Larche) refers to the major ice-free pass across this
 254 sector of the Alps at the YD.
 255

256 *4.3 Palaeo- and present-day climate at the Maritime Alps YD ELA*

257 The YD average T_{Jul} at 2358 ± 15 m asl, the Maritime Alps YD ELA, calculated from the Lago
 258 Piccolo di Avigliana chironomid study (Larocque and Finsinger, 2008), is 3.3 ± 1 °C. The YD average T_{Jan} ,
 259 obtained from the Lago dell’Orgials pollen study (Ortu et al., 2008), is -17.7 ± 0.1 °C, thus defining a
 260 seasonality ($T_{Jul} - T_{Jan}$) of 21.0 °C. With this, it is possible to estimate a T_{melt} of 2.4 ± 1 °C and a P_{ann} of
 261 1549 ± 26 mm/yr, by applying a sine curve to model the monthly air temperature and the Ohmura and
 262 Boettcher (2018) equation.

Glacier name	Longitude (°E)	Latitude (°N)	Area (km ²)	Volume (km ³)	AABR ELA (m asl)	Reconstructed glacier front morphology
Orgials	7.147	44.210	2.231	0.107	2346	Moraine
Aver West	7.137	44.223	0.928	0.037	2346	-
San Giovanni	7.133	44.233	0.755	0.029	2351	-
Maladecia	7.143	44.240	0.641	0.021	2357	-
Argentera	6.942	44.369	1.389	0.080	2359	-
Bandia	7.093	44.378	3.366	0.360	2352	-
Becco Nero	7.075	44.382	1.733	0.360	2373	-
Bernolfo	7.015	44.251	5.991	0.407	2373	Glacial deposit
Bersezio	6.982	44.396	0.632	0.014	2370	-
Ciaval	7.025	44.304	1.655	0.055	2354	Moraine
Guercia	7.050	44.233	0.606	0.025	2369	Glacial deposit
Collalunga - San Bernolfo	7.035	44.232	2.360	0.407	2348	Moraine
Cologna	7.055	44.375	0.563	0.018	2356	-
Fauniera	7.115	44.380	2.314	0.360	2358	-
Ferrere	6.927	44.355	2.897	0.150	2351	moraine
Fornaris	6.945	44.334	3.893	0.195	2349	moraine
Malinvern	7.186	44.211	4.727	0.188	2364	Glacial deposit
Paur	7.203	44.227	1.370	0.052	2367	moraine
Aver East	7.153	44.229	1.669	0.083	2360	-
Perdù	7.201	44.237	0.927	0.031	2357	-
Martel	7.155	44.240	0.473	0.083	2353	Rock glacier
Giordano	7.031	44.368	1.881	0.118	2346	-
Ischiator	7.013	44.277	2.677	0.112	2362	Moirane
Lose	6.931	44.378	0.951	0.034	2361	-
Ciamp	7.195	44.249	0.466	0.015	2348	Glacial deposit
Faniet	6.973	44.341	0.199	0.005	2353	-
Ventasuso	6.903	44.402	0.820	0.030	2358	-
Rocco Verde East	6.977	44.335	0.088	0.001	2355	Glacial deposit
Ciaval South	7.021	44.294	0.104	0.002	2354	Glacial deposit
Saletta	7.033	44.278	0.175	0.004	2357	Moraine
Maladecia west	7.127	44.242	0.088	0.002	2348	-
Cairilliera East	7.154	44.247	0.203	0.005	2354	Moraine
Reduc	7.244	44.262	0.832	0.027	2349	-
Cairilliera West	7.147	44.248	0.046	0.001	2361	-
Bravaria	7.106	44.261	0.166	0.004	2372	Rock glacier
Ciarnier	7.149	44.260	0.047	0.001	2353	Rock glacier
Lausfer	7.092	44.227	0.415	0.020	2364	-
Passo Lausfer	7.083	44.234	0.513	0.018	2371	-
Mouton West	7.089	44.252	0.131	0.004	2346	Rock glacier
Mouton East	7.097	44.248	0.676	0.049	2358	Moraine
Steliere	7.110	44.267	0.064	0.001	2352	Moraine
Pignal	7.063	44.242	0.196	0.004	2351	Moraine
Lake Sauma	7.061	44.245	0.071	0.001	2368	Glacial deposit
Vallonet	7.055	44.244	0.187	0.006	2360	Moraine
Rocca Bernolfo	7.034	44.246	0.251	0.006	2357	Rock glacier
Loroussa South	7.028	44.269	0.109	0.002	2370	Glacial deposit
Cavias	7.041	44.309	0.206	0.007	2349	Rock glacier
Bassura North	6.982	44.345	0.154	0.003	2360	Rock glacier
Moura	7.122	44.348	0.110	0.080	2365	-
Nebius	7.119	44.343	0.122	0.002	2348	-
Oserot	7.006	44.389	3.679	0.241	2373	-
Stau North	6.960	44.335	0.427	0.022	2352	Moraine
Pilone	6.965	44.337	0.289	0.022	2369	Moraine
Peroni	6.966	44.402	1.541	0.146	2372	-
Piz	6.995	44.297	5.657	0.381	2370	-
Ponte Bernardo	6.969	44.304	1.600	0.043	2371	-
Puriac	6.908	44.375	6.373	0.373	2347	Glacial deposit
Roburent	6.943	44.415	3.363	0.155	2362	-
Nebius North	7.114	44.351	0.450	0.080	2349	-
Scoletta	6.984	44.306	0.643	0.016	2355	-
Serour	7.120	44.361	0.174	0.005	2366	-
Tesina	7.067	44.235	1.216	0.057	2354	Moraine
Valletta	7.212	44.248	2.839	0.168	2349	Moraine
Panieris	6.964	44.319	1.111	0.037	2368	-
Stau	6.967	44.328	0.969	0.018	2353	-
Vallonetto	7.048	44.368	0.346	0.007	2373	Moraine
TOTAL	-	-	83.743	5.394	-	-

263

264

265

266

Table 2 Name, midpoint coordinates, area, volume and ELA of 66 reconstructed YD glaciers in the Stura catchment. The presence of a moraine, a rock glacier, or generic glacial deposit at the reconstructed glacier front is also noted.

267

268 The present-day (2001-2018) precipitation at the nearby Diga del Chiotas weather station (1980 m asl,
269 i.e. 378 m lower than the YD ELA) is 1487 mm/yr and the January, July and summer (June-August)
270 temperatures are -1.7°C, 13.8°C and 12.8°C, respectively. These temperatures, when adjusted to the
271 elevation of the YD average ELA using the standard lapse rate, return values of -2.8°C, 11.4°C and
272 10.4°C respectively, with a seasonality of 14.2°C.

273

274 5. Discussion

275 Well-preserved moraines associated with the Egesen stadial, the last of the Lateglacial stadials
276 in the European Alps, are common (Ivy Ochs et al., 2009). They are recognised as the first prominent,
277 blocky, usually multi-crested moraine set that can be found downvalley from the Little Ice Age moraine
278 (Ivy-Ochs, 2015). The FER moraine fits this description: it is the first moraine set that can be found
279 (about 2 km) downvalley from the Holocene moraines in the Val Forneris; its aspect, characterised by
280 very large boulders, resembles that of many other Alpine Egesen moraines (see Figure 4 in Hormes et
281 al., 2008); the presence of nearby moraines, most likely connected to the same climatic event, is also
282 a typical trait of the Egesen geomorphological signature across the Alps (Ivy Ochs, 2015). A handful of
283 Egesen stadial moraines has so far been dated with cosmogenic isotope exposure dating techniques,
284 all returning an age compatible with the YD (Baroni et al., 2017; Böhlert et al., 2011a; Cossart et al.,
285 2012; Federici et al., 2008; Hormes et al., 2008; Ivy-Ochs et al., 1996; 2006; 2009; Kelly et al., 2004;
286 Moran et al., 2016; Schindelwig et al., 2012). The FER moraine, dated here to the YD, is an important
287 addition to this sparse database. It provides further evidence that the Egesen stadial in the European
288 Alps actually represents the glaciological and morphological expression of the YD cooling event. It also
289 allows for the reconstruction of several potential YD/Egesen glaciers within its neighbourhood and its
290 ELA can be used to extract YD climatic conditions in this sector of the Alps.

291

292 5.1 Climate

293 A proper comparison of ELA values across the Alps for the YD is beyond the scope of this work
294 and would require a consistent reconstruction of all YD palaeoglaciers and the extraction of their ELA
295 with a same approach. However, different ELA calculation approaches would typically account for ELA
296 discrepancy of the order of some tens of meters, for alpine valley glaciers of the size considered here
297 (e.g. Federici et al., 2017; Scotti et al., 2017). The average ELA (2358 m asl) of the two YD reconstructed
298 glaciers of the Maritime Alps is a few hundred meters lower than the ELA reported from other Alpine
299 sectors for this same glacier stadial (Baroni et al., 2017; Scotti et al., 2017). This difference is an order
300 of magnitude greater than a potential methodologically-related discrepancy, indicating that the
301 climatic conditions of the Maritime Alps at the YD were peculiar within the context of the Alps. In an

302 alpine environment, the ELA of a valley glacier is largely controlled by the summer temperature, which
303 influences glacier ablation; and by solid, typically winter, precipitation, which affects ice accumulation.
304 The lower YD ELA of the Maritime Alps therefore reflects lower summer temperature and/or higher
305 solid precipitation, relative to the rest of the Alps.

306 The climatic reconstruction attempted here shows increased seasonality (6.8°C higher,
307 relative to present-day measurements) and a considerable drop in temperature at the YD (8.1°C lower
308 in July and 14.9°C lower in January, relative to present-day measurements), in line with other Alpine
309 YD palaeoclimate studies (e.g. [Lotter et al., 2000](#); [Heiri et al., 2014b](#)). However, it is the relatively high
310 YD precipitation, comparable to the present-day precipitation, that makes the YD climate of the
311 Maritime Alps peculiar within the context of the wider Alps. This is in apparent disagreement with the
312 paradigm of a widespread arid YD across most of Europe and the Alps (e.g. [Heiri et al., 2014a and b](#);
313 [Magny et al., 2001](#)), including its SW sector ([Ortu et al., 2008](#); [Brisset et al., 2015](#)); however, a previous
314 attempt to reconstruct palaeoprecipitation based on YD glacier ELA has highlighted considerable
315 variability in the central Alps, including regions where YD precipitation was similar to, and even higher
316 than, present-day precipitation ([Kerschner, 1981](#); [Kerschner et al., 2000](#); [Kerschner & Ivy-Ochs, 2008](#)).

317 The Maritime Alps YD climate reconstruction is based on at least three aspects that can be
318 challenged. Firstly, the YD relationship between temperature and precipitation at the ELA may have
319 been different from today's. Nonetheless, it is hard to physically justify such a scenario, as the law is
320 robustly based on current worldwide empirical observations, not specific to an individual site and
321 considering multi-decadal data ([Ohmura and Boettcher, 2018](#)). Secondly, the chironomid-derived YD
322 T_{Jul} might reflect local conditions only, thus questioning its validity for the calculation of temperatures
323 for a site that is 95 km away and at an elevation almost 2000 m higher. Thirdly, the pollen-derived YD
324 T_{Jan} , although relative to a site located within the Maritime Alps and at an elevation similar to the YD
325 ELA, might not be reliable since the approach suffers from lack of good analogues, problems with
326 pollen taxa and complexity of mountain ecosystems (e.g. [Ortu et al., 2006](#)). Despite these potential
327 limitations, it should be noted that a recent study, based on fossil trees from a location ~90 km west
328 of our site, also indicates non-arid conditions for this region at the onset of the YD ([Pauly et al., 2018](#)).
329 These conditions are interpreted as the effect of more frequent and/or intense precipitations
330 originating from North Atlantic air masses, combined with more intense winter storms resulting from
331 the interaction between cold high-latitude and warm Mediterranean air masses, along the margin of
332 the southward-displaced polar front ([Pauly et al., 2018](#)). Such an interpretation fits very well with the
333 uniqueness of the Maritime Alps YD glaciers within the context of the wider Alpine region, because of
334 their closer proximity to both the Mediterranean Sea and the Atlantic Ocean.

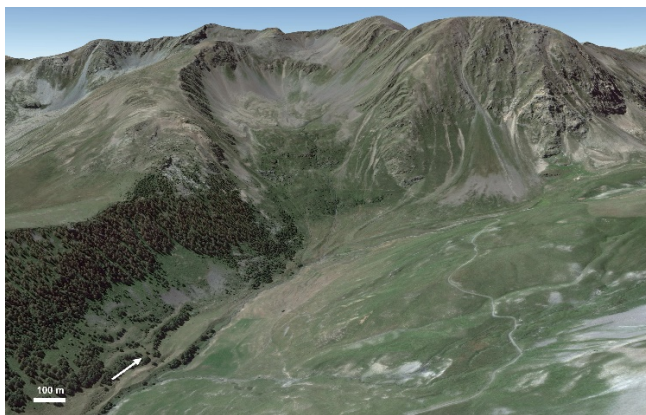
335

336 *5.2 Regional glaciers reconstruction*

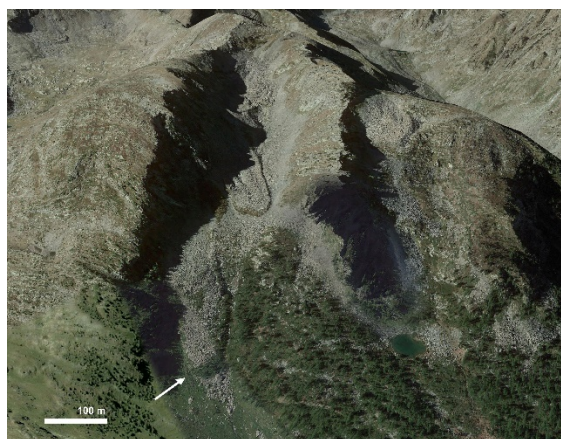
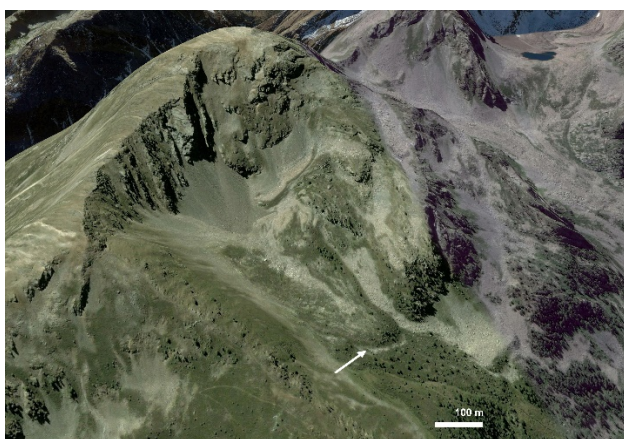
337 This paper represents the first attempt at using the GIS GlaRe tool ([Pellitero et al., 2016](#)) to model the
338 extent of all palaeoglaciers belonging to the same stadial in an extensive alpine region, using the ELA
339 of nearby palaeoglaciers associated with moraines also dated to that stadial. Although the trial-and-
340 error approach (by iteration of the glacier front position) is time-consuming, the reconstruction of 66
341 glaciers took some weeks against the months it would have probably taken using the classic manual
342 topographic approach (e.g. [Porter et al., 1975](#); [Carr et al., 2010](#)), i.e. without the use of GlaRe. Most
343 importantly, GlaRe implements a physically-plausible plastic rheology glacier model for the glacier
344 reconstruction, thus giving further robustness to the results. The application of a regional ELA interval
345 defined by two dated moraines is questionable, since it is possible that ELA variability exceeded these
346 boundaries across the 66 glaciers. However, the defined interval allows us to provide a first order
347 model of the YD expansion and could be useful for further, more detailed studies.

348

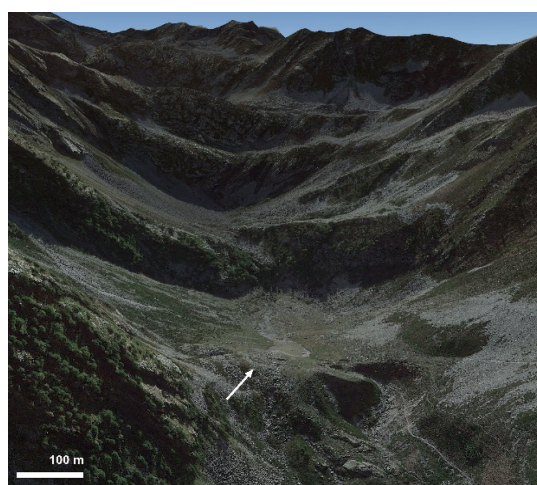
349



350



351



352 Figure 4. Examples of identified moraines on Google Earth™ located at the front (ice margin) of the
353 reconstructed YD glaciers in the Stura catchments. Top left: Ferrere glacier (the approximate coordinates of the
354 moraine are 44.35°N, 6.95°E); Top right: Laorussa South glacier (44.27°N, 7.03°E); Centre left: Saletta glacier
355 (44.28°N, 7.03°E); centre right: Pignal glacier (44.25°N, 7.07°E); Bottom left: Maladecia glacier (44.24°N, 7.14°E);
356 Bottom right: Valletta glacier (44.26°N, 7.21°E).

357
358 In order to test the modelled reconstruction presented here, the location of the 66-glacier
359 front was checked in Google Earth™ and on an available geology map of the region that include some
360 surface geology (Malaroda et al., 1970), with the aim to find evidence of a frontal moraine (Table 2).
361 Twenty-nine percent of the settings have evidence of a moraine (Figure 4), while another 14% include
362 glacial deposits where the morphology of a moraine could not be determined for sure, possibly an

363 issue related to the resolution of the available images. In some instances (another ~10% of the cases),
364 a rock glacier is found in the vicinity of the reconstructed glacier front, possibly incorporating a
365 potential YD moraine. This is in line with the evidence that the activity of many rock glaciers in the
366 Alps can be traced back to the end of the YD (Ivy-Ochs et al., 2009; Böhlert et al., 2011b; Moran et al.,
367 2016). The remaining 47% of reconstructed glaciers are characterised by the absence of a moraine or
368 a rock glacier at their front: in many instances, the resolution of the available imagery is either not
369 sufficiently high for the task, or the potential frontal moraine area is covered by thick vegetation. In
370 other, locations are clearly unsuitable for the deposition or preservation of a moraine, because the
371 valley bottom is particularly steep. If a moraine has not been identified, despite a favourable setting
372 and good imagery, the deposit might have been eroded by post-glacial events, buried by fluvial or
373 scree deposition. It is also possible that microclimatic conditions (e.g. those related to aspect) might
374 have resulted in a slightly longer or shorter glacier than the reconstructed one which is based on a
375 regional ELA and obtained using a tool, GlaRe, that does not take into consideration valley aspect. In
376 the future, it would be interesting to improve testing by undertaking extensive field work to verify all
377 the percentages reported above and by exposure-dating the moraines that will be identified.
378 However, for the time being, it is encouraging to see that several potential YD moraines are present
379 in the location identified by our modelled reconstruction (Table 2; Figure 4). This suggests that GlaRe
380 could be used as a predictive tool for further geomorphological investigations specific to a glacial
381 stadial for which at least one, ideally some, reliable (i.e. connected to a dated moraine) glacier
382 reconstructions and ELA calculations are available within a same region. For example, this could be
383 very helpful to plan fieldwork aimed at reaching other glacier front sites in nearby valleys, where
384 potential moraines of the same age could be found, sampled and dated.

385 YD glacier expansion in the Stura catchment sector of the Alps was limited to about 6% of the
386 total catchment area and confined to the highest altitudes, between 1596 and 2893 m asl. This is a
387 considerable reduction when compared to the Last Glacial Maximum expansion, when the Stura, like
388 other nearby major catchments, was occupied by a system of interconnected glaciers covering most
389 of the catchment and extending downvalley to the mountain front at 700 m asl, i.e. almost reaching
390 the Po Plain (Federici et al., 2008, 2012, 2017). Our modelled reconstruction indicates that most YD
391 glaciers extended hundreds of metres up to a few kilometres beyond the cirques. Some neighbouring
392 valley glaciers were connected, but not extensively enough to justify a description of the Egesen glacial
393 stadial in the Maritime Alps as an ice field. Almost all Stura valleys were glaciated at the YD, thus
394 considerably limiting plant/animal/human interaction, migration, communication and trading
395 between the southern and norther sectors of this Alpine region. The configuration of the YD Stura
396 glaciers indicates that only one pass across the main Alpine divide was then ice-free, the

397 Maddalena/Larche (44.42°N, 6.90°E, 1996 m asl). This was most-likely due to its elevation, which is at
398 least 300 m lower than all other main divide passes along the Stura valleys, associated with a lack of
399 nearby, high-elevation valleys and peaks that could have sustained a glacier able to reach the pass.
400 Ice-free Alpine passes are known to have played a crucial role in influencing pastoralism and
401 transhumance in the Alps during the early Holocene (e.g. [Hafner and Schwörer, 2018](#)) and it is likely
402 that they also played a role in influencing YD human activity, typically hunting and gathering. While
403 there is only limited information available on early human presence in the Alps, evidence of YD
404 settlements (campsites) generally linked to seasonal hunting has been recorded from various Alpine
405 archaeological sites ([Mussi and Persani, 2011](#); [Weber et al., 2011](#)), including the Maritime Alps
406 ([Tzortzis et al., 2008](#)). Within this sector of the mountain chain, it is likely that human (and animal)
407 interaction and migration across the Alpine main divide during the YD were funnelled in the
408 Maddalena/Larche pass. This represents an ideal site for future palaeoecological, palaeozoological
409 and archaeological investigations.

410

411 6. Conclusions

- 412 • A new Egesen stadial moraine in the Maritime Alps is dated here to $12,950 \pm 700$ yr (weighted
413 mean value of three measurements \pm weighted standard deviation) by means of cosmogenic
414 isotope analysis, thus adding further evidence to the link between the Egesen stadial of the
415 European Alps and the YD cooling event.
- 416 • The YD glacier that deposited the moraine is reconstructed and its ELA calculated to 2349 ± 5
417 m asl. This value is very similar to the ELA (2368 ± 5 m asl) of another palaeoglacier that
418 deposited a moraine (PDP) dated to the YD, 40 km to the SW. The similarity between the two
419 ELA suggests that the region experienced similar climatic conditions during the YD.
- 420 • The average between the two ELAs (2358 ± 15 m asl), combined with palaeotemperature data
421 provided by independent proxies, is used to establish the Maritime Alps YD annual
422 precipitation at the ELA, 1549 ± 26 mm/yr, based on the empirical law that links temperature
423 and precipitation at the ELA. Unlike most other Alpine sectors and European regions where
424 the YD seems to be characterised by aridity, the reconstructed YD precipitation for the
425 Maritime Alps is similar to present-day precipitation. This peculiarity is most likely related to
426 the Maritime Alps crossroads position, which allowed the region to intercept cold and humid
427 air masses from the Atlantic Ocean, pushed south by the displaced polar front, and warm and
428 humid air masses from the nearby Mediterranean Sea.
- 429 • The YD ELA interval defined by the two dated moraines allows to model the extent of all
430 potential YD glaciers (66) in the Stura catchment. The modelled location of the glaciers' front
431 matched well with the position of actual frontal moraine and glacial deposits observed in the

432 valleys, thus demonstrating that GLARE can be used as a predictive, modelling tool. The
433 modelled glaciers occupied all valley heads in the catchment with only one notable ice-free
434 pass across the main Alpine divide, that of the Maddalena/Larche pass. This is an ideal site for
435 future archaeological, palaeocological and palaeozoological studies with a focus on YD cross-
436 Alpine interactions in the Maritime Alps.

437

438

439 ACKNOWLEDGEMENTS

440 We would like to acknowledge: Prof. Rea and Dr Pellitero for fruitful discussions on various aspects of this
441 work, and in particular on the use of glacier reconstruction and ELA GIS tools and extraction of climatic
442 variables at a glacier ELA; Dr Ortu for kindly providing easy access to pollen data and for discussions on the
443 climate of the Younger Dryas across the Alps; Prof. Edwards for discussions on pollen analyses; and Prof.
444 Federici, for inspiring glaciological research in this beautiful region. The constructive and useful feedback
445 provided by Dr Monegato and an anonymous reviewer is greatly appreciated. L. Cignoni is thanked for
446 reviewing the English. MS acknowledges support from NERC (CIAF 9092.1010).

447

448 REFERENCES

449 Auer, I., Böhm, R., Jurkovic, A., Lipa, W., Orlik, A., Potzmann, R., Schöner, W., Ungersböck, M., Matulla,
450 C., Briffa, K., Jones, P. D., Efthymiadis, D., Brunetti, M., Nanni, T., Maugeri, M., Mercalli, L., Mestre, O.,
451 Moisselin, J.-M., Begert, M., Müller-Westermeier, G., Kveton, V., Bochnicek, O., Stastny, P., Lapin, M.,
452 Szalai, S., Szentimrey, T., Cegnar, T., Dolinar, M., Gajic-Capka, M., Zaninovic, K., Majstorovic, Z.,
453 Nieplova, E., 2007. HISTALP — 'Historical instrumental climatological surface time series of the Greater
454 Alpine Region 1760–2003'. *Int. J. Climatol.* 27, 17–46.

455 Badino, F., Ravazzi, C., Vallè, F., Pini, R., Aceti, A., Brunetti, M., Champvillair, E., Maggi, V., Maspero,
456 F., Perego, R., Orombelli, G., 2018. 8800 years of high-altitude vegetation and climate history at the
457 Rutor Glacier forefield, Italian Alps. Evidence of middle Holocene timberline rise and glacier
458 contraction. *Quat. Sci. Rev.* 185, 41–68.

459 Baroni, C., Casale, S., Salvatore, M.C., Ivy-Ochs, S., Christl, M., Carturan, L., Seppi, R., Carton, A., 2017.
460 Double response of glaciers in the Upper Peio Valley (Rhaetian Alps, Italy) to the Younger Dryas
461 climatic deterioration. *Boreas* 46, 783–798.

462 Benn, D.I., Hulton, N.R.J., 2010. An Excel™ spreadsheet program for reconstructing the surface
463 profile of former mountain glaciers and ice caps. *Comput. Geosci.* 36, 605–610.

464 Benn, D.I., Lehmkuhl, F., 2000. Mass balance and equilibrium line altitudes of glaciers in high mountain
465 environments. *Quat. Int.* 65, 15–29.

466 Bigot-Cormier, F., Braucher, R., Bourlès, D., Guglielmi, Y., Dubar, M., Stéphan, J.F., 2005. Chronological
467 constraints on processes leading to large active landslides. *Earth Planet. Sci. Lett.* 235, 141–150.

468 Bini, A., Buoncristiani, J.-F., Couterrand, S., Ellwanger, D., Felber, M., Florineth, D., Graf, H.R., Keller,
469 O., Kelly, M., Schlüchter, C., Schoeneich, P., 2009. Die Schweiz Während des Letzzeitlichen
470 Maximums (LGM) 1:500 000. Federal Office of Topography, swisstopo, Wabern, Switzerland.

471 Böhlert, R., Egli, M., Maisch, M., Brandová, D., Ivy-Ochs, S., Kubik, P.W., Haeberli, W., 2011a.
472 Application of a combination of dating techniques to reconstruct the Lateglacial and early Holocene
473 landscape history of the Albula region (eastern Switzerland). *Geomorphology* 127, 1-13.

474 Böhlert, R., Compeer, M., Egli, M., Brandova, D., Maisch, M., Kubik, P.W., Haeberli, W., 2011b. A
475 combination of relative-numerical dating methods indicates two high Alpine rock glacier activity
476 phases after the glacier advance of the Younger Dryas. *Open Geogr. J.* 4, 115-130.

477 Boston, C. M., Lukas, S., Carr, S. J., 2015. A Younger Dryas plateau icefield in the Monadhliath, Scotland,
478 and implications for regional palaeoclimate. *Quat. Sci. Rev.* 108, 139-162

479 Brisset, E., Guiter, F., Miramont, C., Revel, M., Anthony, E. J., Delhon, C., Arnaud, F., Malet, E., de
480 Beaulieu, J.L., 2015. Lateglacial/Holocene environmental changes in the Mediterranean Alps inferred
481 from lacustrine sediments. *Quat. Sci. Rev.*, 110, 49-71.

482 Broecker, W.S., Denton, G.H., Edwards, R.L., Cheng, H., Alley, R.B., Putnam A.E., 2010. Putting the
483 Younger Dryas cold event into context. *Quat. Sci. Rev.* 29, 1078–1081.

484 Brugger, K.A., 2006. Late Pleistocene climate inferred from the reconstruction of the Taylor River
485 glacier complex, southern Sawatch Range, Colorado. *Geomorphol.* 75, 318-329

486 Cacho, I., Grimalt, J.O., Canals, M., Sbaffi, L., Shackleton, N.J., Schönfeld, J., Zahn, R., 2001. Variability
487 of the Western Mediterranean sea surface temperature during the last 25,000 years and its
488 connection with the Northern Hemisphere climatic changes. *Paleoceanography* 16, 40-52.

489 Carr, S.J., Lukas, S., Mills, S.C., 2010. Glacier reconstruction and mass-balance modelling as a
490 geomorphic and palaeoclimatic tool. *Earth Surf. Processes Landf.* 35, 1103-1115.

491 Casazza, G., Grassi, F., Zecca, G., Minuto, L., 2016. Phylogeographic Insights into a peripheral refugium:
492 the importance of cumulative effect of glaciation on the genetic structure of two endemic plants. *PLoS*
493 *One* 11, e0166983.

494 Clark, P.U., Dyke, A.S., Shakun, J.D., Carlson, A.E., Clark, J., Wohlfarth, B., Mitrovica, J.X., Hostetler,
495 S.W., McCabe, A.M., 2009. The Last Glacial Maximum. *Science* 325, 710-714.

496 Catto, N., Liverman, D.G.E., Bobrowsky, P.T., Rutter, N., 1996. Laurentide, cordilleran, and montane
497 glaciation in the western Peace River - Grande Prairie region, Alberta and British Columbia, Canada.
498 *Quat. Int.* 32, 21-32.

499 Cossart, E., Fort, M., Boursès, D., Braucher, R., Perrier, R., Siame, L., 2012. Deglaciation pattern during
500 the Lateglacial/Holocene transition in the southern French Alps. Chronological data and geographical
501 reconstruction from the Clarée Valley (upper Durance catchment, southeastern France). *Palaeogeogr.,*
502 *Palaeoclimatol., Palaeoecol.* 315, 109-123.

503 Durand, Y., Laternser, M., Giraud, G., Etchevers, P., Lesaffre, B., Mérindol, L., 2009. Reanalysis of 44 yr
504 of climate in the French Alps (1958–2002): methodology, model validation, climatology, and trends
505 for air temperature and precipitation. *J. Appl. Meteorol. Climatol.* 48, 429–449.

506 Ehlers, J., Gibbard, P.L., 2004. Quaternary glaciations—extent and chronology: Part I: Europe. Elsevier,
507 Amsterdam.

508 Federici, P.R., Pappalardo, M., Ribolini, A., 2003. Geomorphological map of the Maritime Alps Natural
509 Park (Argentera Massif, Italy) and surroundings. Colour map, 1:25.000 scale, S.EL.CA., Firenze.

- 510 Federici, P.R., Granger, D.E., Pappalardo, M., Ribolini, A., Spagnolo, M., Cyr, A. J., 2008. Exposure age
511 dating and Equilibrium Line Altitude reconstruction of an Egesen moraine in the Maritime Alps, Italy.
512 *Boreas* 37, 245–253.
- 513 Federici, P.R., Granger, D.E., Ribolini, A., Spagnolo, M., Pappalardo, M., Cyr, A.J., 2012. Last Glacial
514 Maximum and the Gschnitz stadial in the Maritime Alps according to ¹⁰Be cosmogenic dating. *Boreas*
515 41, 277-291.
- 516 Federici, P.R., Ribolini, A., Spagnolo, M., 2017. Glacial history of the Maritime Alps from the Last Glacial
517 Maximum to the Little Ice Age. *Geol. Soc. London, Special Publication* 433, 137–159.
- 518 Florineth, D., Schlüchter, C., 1998. Reconstructing the Last Glacial Maximum (LGM) ice surface
519 geometry and flowlines in the Central Swiss Alps. *Eclogae Geol. Helv.* 91, 391–407.
- 520 Furbish, D.J., Andrews, J.T., 1984. The use of hypsometry to indicate long term stability and response
521 of valley glaciers to changes in mass transfer. *J. Glaciol.* 30, 199–211.
- 522 Garnier, S., Alibert, P., Audiot, P., Prieur, B., Rasplus, J.-Y., 2004. Isolation by distance and sharp
523 discontinuities in gene frequencies: Implications for the phylogeography of an alpine insect species,
524 *Carabus solieri*. *Mol. Ecol.* 13, 1883-1897.
- 525 Golledge, N.R., Hubbard, A., Sugden, D.E., 2008. High-resolution numerical simulation of Younger
526 Dryas glaciation in Scotland. *Quat. Sci. Rev.* 27, 888-904.
- 527 Hafner, A., Schwörer, C., 2018. Vertical mobility around the high-alpine Schnidejoch Pass. Indications
528 of Neolithic and Bronze Age pastoralism in the Swiss Alps from paleoecological and archaeological
529 sources. *Quat. Int.* 484, 3-18.
- 530 Heiri, O., Brooks, S.J., Renssen, H., Bedford, A., Hazekamp, M., Ilyashuk, B., Jeffers, E.S., Lang, B.,
531 Kirilova, E., Kuiper, S., Millet, L., Samartin, S., Toth, M., Verbruggen, F., Watson, J.E., Van Asch, N.,
532 Lammertsma, E., Amon, L., Birks, H.H., Birks, H.J.B., Mortensen, M.F., Hoek, W.Z., Magyari, E., Munõz
533 Sobrino, C., Seppä, H., Tinner, W., Tonkov, S., Veski, S., Lotter, A.F., 2014a. Validation of climate model-
534 inferred regional temperature change for lateglacial Europe. *Nat. Comm.* 5, 4914.
- 535 Heiri, O., Koinig, K.A., Spötl, C., Barrett, S., Brauer, A., Drescher-Schneider, R., Gaar, D., Ivy-Ochs, S.,
536 Kerschner, H., Luetscher, M., Moran, A., Nicolussi, K., Preusser, F., Schmidt, R., Schoeneich, P.,
537 Schwörer, C., Sprafke, T., Terhorst, B., Tinner, W., 2014b. Palaeoclimate records 60-8 ka in the Austrian
538 and Swiss Alps and their forelands. *Quat. Sci. Rev.* 106, 186-205.
- 539 Heuberger, H., 1968. Die Alpengletscher im Spät- und Postglazial. *Eiszeitalter und Gegenwart* 19, 270–
540 275.
- 541 Hormes, A., Ivy-Och, S., Kubik, P.W., Ferreli, L., Michetti, A.M., 2008. ¹⁰Be exposure ages of a rock
542 avalanche and a late glacial moraine in Alta Valtellina, Italian Alps. *Quat. Int.* 190, 136–145.
- 543 Hughes, P.D., Braithwaite, R., 2008. Application of a degree-day model to reconstruct Pleistocene
544 glacial climates. *Quat. Res.* 69, 110-116.
- 545 Hughes, P.D., Gibbard, P.L., Ehlers, J., 2013. Timing of glaciation during the last glacial cycle: evaluating
546 the concept of a global ‘Last Glacial Maximum’ (LGM). *Earth-Sci. Rev.* 125, 171-198.
- 547 Hughes, P.D., Woodward, J.C., Gibbard, P.L., 2007. Middle Pleistocene cold stage climates in the
548 Mediterranean: new evidence from the glacial record. *Earth Planet. Sci. Lett.* 253, 50–56.

549 Isola, I., Ribolini, A., Zanchetta, G., Bini, M., Regattieri, E., Drysdale, R.N., Hellstrom, J.C., Bajo, P.,
550 Montagna, P., Pons-Branchu, E., 2019. Speleothem U/Th age constraints for the Last Glacial conditions
551 in the Apuan Alps, northwestern Italy. *Palaeogeog. Palaeoclimatol. Palaeoecol.* 518, 62-71

552 Isotta, F.A., Frei, C., Weilguni, V., Perčec Tadić, M., Lassègues, P., Rudolf, B., Pavan, V., Cacciamani,
553 C., Antolini, G., Ratto, S. M., Munari, M., Micheletti, S., Bonati, V., Lussana, C., Ronchi, C., Panettieri,
554 E., Marigo, G., Vertačnik, G., 2014. The climate of daily precipitation in the Alps: development and
555 analysis of a high-resolution grid dataset from pan-Alpine rain-gauge data. *Int. J. Climatol.* 34, 1657-
556 1675.

557 Ivy-Ochs, S. 2015. Glacier variations in the European Alps at the end of the last glaciation. *Cuad. Invest.*
558 *Geogr.* 41, 295– 315.

559 Ivy-Ochs, S., Schlüchter, C., Kubik, P. W., Synal, H.-A., Beer, J., Kerschner, H., 1996. The exposure age
560 of an Egesen moraine at Julier Pass, Switzerland, measured with the cosmogenic radionuclides ^{10}Be ,
561 ^{26}Al and ^{36}Cl . *Eclogae Geol. Helv.* 89, 1049–1063.

562 Ivy-Ochs, S., Kerschner, H., Reuther, A., Maisch, M., Sailer, R., Schaefer, J., Kubik, P.W., Synal, H.A.,
563 Schlüchter, C., 2006. The timing of glacier advances in the northern European Alps based on surface
564 exposure dating with cosmogenic ^{10}Be , ^{26}Al , ^{36}Cl , and ^{21}Ne . In: Siame, L.L., Bourle`s, D.L., Brown, E.T.
565 (Eds.), *In Situ-Produced Cosmogenic Nuclides and Quantification of Geological Processes*. *Geol. Soc.*
566 *Am. Special Paper* 415, pp. 43–60.

567 Ivy-Ochs, S., Kerschner, H., Maisch, M., Christl, M., Kubik, P. W., Schlüchter, C., 2009. Latest Pleistocene
568 and Holocene glacier variations in the European Alps. *Quat. Sci. Rev.* 28,
569 2137–2149.

570 Kelly, M.A., Kubik, P.W., Von Blankenburg, F., Schlüchter, C. 2004. Surface exposure dating of the Great
571 Aletsch Glacier Egesen moraine system, western Swiss Alps, using the cosmogenic nuclide ^{10}Be . *J.*
572 *Quat. Sci.* 19, 431–441.

573 Kerschner, H. 1981. Outlines of the climate during the Egesen Advance (Younger Dryas, 1000-10000
574 BP) in the central Alps of the western Tyrol, Austria. *Z. Gletscherkd. Glazialgeol.* 16, 229-240.

575 Kerschner, H., Kaser, G., Sailer, R., 2000. Alpine Younger Dryas glaciers as paleo-precipitation gauges.
576 *Ann. Glaciol.* 31, 80–84.

577 Kerschner, H., Ivy-Ochs, S., 2008. Palaeoclimate from glaciers: Examples from the Eastern Alps during
578 the Alpine Lateglacial and early Holocene. *Glob. Planet. Chang.* 60, 58-71.

579 Kohl, C.P., Nishiizumi, K., 1992. Chemical isolation of quartz for measurement of in-situ -produced
580 cosmogenic nuclides. *Geochim. Cosmochim. Acta* 56, 3583-3587.

581 Johnsen, S.J., Dahl-Jensen, D., Gundestrup, N., Steffensen, J.P., Clausen, H.B., Miller, H., Masson-
582 Delmotte, V., Sveinbjörnsdottir, A.E., White, J., 2001. Oxygen isotope and palaeotemperature records
583 from six Greenland ice-core stations: Camp Century, Dye-3, GRIP, GISP2, Renland and NorthGRIP. *J.*
584 *Quat. Sci.* 16, 299–307.

585 Jones, R.S., Small, D., Cahill, N., Bentley, M.J., Whitehouse, P.L., 2019. iceTEA: Tools for plotting and
586 analysing cosmogenic-nuclide surface-exposure data from former ice margins. *Quat. Geochronol.* 51,
587 72-86.

- 588 Larocque, I., Finsinger, W., 2008. Late-glacial chironomid-based temperature reconstructions for Lago
589 Piccolo di Avigliana in the southwestern Alps (Italy). *Palaeogeogr. Palaeoclimatol. Palaeoecol.* 257,
590 207–223.
- 591 Lotter, A.F., Birks, H.J.B., Eicher, U., Hofmann, W., Schwander, J., Wick, L., 2000. Younger Dryas and
592 Allerod summer temperatures at Gerzensee (Switzerland) inferred from fossil pollen and cladoceran
593 assemblages. *Palaeogeogr., Palaeoclimatol., Palaeoecol.* 159, 349-361.
- 594 Magny, M., Guiot, J., Schoellammer, P., 2001. Quantitative Reconstruction of Younger Dryas to Mid-
595 Holocene Paleoclimates at Le Locle, Swiss Jura, Using Pollen and Lake-Level Data. *Quat. Res.* 56, 170-
596 180.
- 597 Malaroda, R., Carraro, F., Dal Piaz, G.B., Franceschetti, B., Sturani, C., Zanella, E., 1970. Carta Geologica
598 del Massiccio dell'Argentera alla scala 1:50 000 e Note Illustrative. *Mem. Soc. Geol. Ital.* 9, 557–663.
- 599 Meyer, M.C., Hofmann, Ch.-Ch., Gemell, A.M.D., Haslinger, E., Häusler, H., Wangda, D., 2009.
600 Holocene glacier fluctuations and migration of Neolithic yak pastoralists into the high valleys of
601 northwest Bhutan. *Quat. Sci. Rev.* 28, 1217-1237.
- 602 Moran, A.P., Ivy-Ochs, S., Schuh, M., Christl, M., Kerschner, H., 2016. Evidence of central Alpine glacier
603 advances during the Younger Dryas-early Holocene transition period. *Boreas* 45, 398–410.
- 604 Mussi, M., Peresani, M., 2011. Human settlement of Italy during the Younger Dryas. *Quat. Int.* 242.
605 360-370.
- 606 Musumeci, G., Ribolini, A., Spagnolo, M., 2003. The effects of late Alpine tectonics in the morphology
607 of the Argentera Massif (Western Alps, Italy–France). *Quat. Int.* 101, 191–201.
- 608 Nishiizumi, K., Imamura, M., Caffee, M.W., Southon, J.R., Finkel, R.C., McAninch, J., 2007. Absolute
609 calibration of ¹⁰Be AMS standards. *Nucl. Instrum. Methods Phys. Res. B* 258, 403–413.
- 610 Ohmura, A., Kasser, P., Funk, M., 1992. Climate at the equilibrium line of glaciers. *J. Glaciol.* 38, 397–
611 411.
- 612 Ohmura, A., Boettcher, M., 2018. Climate on the equilibrium line altitudes of glaciers: theoretical
613 background behind Ahlmann's P/T diagram. *J. Glaciol.* 64, 489-505.
- 614 Ortu, E., Brewer, S., Peyron, O., 2006. Pollen-inferred palaeoclimate reconstructions in mountain
615 areas: Problems and perspectives. *J. Quat. Sci.* 21, 615-627.
- 616 Ortu, E., Peyron, O., Bordon, A., de Beaulieu, J.L., Siniscalco, C., Caramiello, R., 2008. Lateglacial and
617 Holocene climate oscillations in the South-western Alps: An attempt at quantitative reconstruction.
618 *Quat. Int.* 190, 71-88.
- 619 Osmaston, H., 2005. Estimates of glacier equilibrium line altitudes by the area_altitude, the
620 area_altitude balance ratio and the area_altitude balance index methods and their validation. *Quat.*
621 *Int.* 138, 22–31.
- 622 Paterson, W.S.B., 1994. *The Physics of Glaciers*, 3rd Edition Pergamon/Elsevier, London.
- 623 Patzelt, G., 1972. Die spätglazialen Stadien und postglazialen Schwankungen von Ostalpengletschern.
624 *Berichte der Deutschen Botanischen Gesellschaft* 85, 47-57.

625 Pauly, M., Helle, G., Miramont, C., Büntgen, U., Treydte, K., Reinig, F., Guibal, F., Sivan, O., Heinrich, I.,
626 Riedel, F., Kromer, B., Balanzategui, D., Wacker, L., Sookdeo, A., Brauer, A., 2018. Subfossil trees
627 suggest enhanced Mediterranean hydroclimate variability at the onset of the Younger Dryas. *Sci. Rep.*
628 *8*, 13980.

629 Pellitero, R., Rea, B.R., Spagnolo, M., Bakke, J., Hughes, P., Ivy-Ochs, S., Lukas, S., Ribolini, A., 2015. A
630 GIS tool for automatic calculation of glacier equilibrium-line altitudes. *Comput. Geosci.* *82*, 55-62.

631 Pellitero, R., Rea, B.R., Spagnolo, M., Bakke, J., Ivy-Ochs, S., Frew, C.R., Hughes, P., Ribolini, A., Lukas,
632 S., Renssen, H., 2016. GlaRe, a GIS tool to reconstruct the 3D surface of palaeoglaciers. *Comput.*
633 *Geosci.* *94*, 77-85.

634 Porter, S.C., 1975. Equilibrium line altitudes of late Quaternary glaciers in the Southern Alps, New
635 Zealand. *Quat. Res.* *5*, 27–47.

636 Ravazzi, C., Peresani, M., Pini, R., Vescovi, E., 2007. The Late Glacial in the Italian Alps and in the Po
637 Plain: Stratigraphy, vegetation history and human peopling [Il Tardoglaciale nelle Alpi e in Pianura
638 Padana. *Evoluzione stratigrafica, storia della vegetazione e del popolamento antropico*]. *Alpine*
639 *Mediterr. Q.* *20*, 163-184.

640 Renssen, H., Mairesse, A., Goosse, H., Mathiot, P., Heiri, O., Roche, D.M., Nisancioglu, K.H., Valdes,
641 P.J., 2015. Multiple causes of the Younger Dryas cold period. *Nat. Geo.* *8*, 946-949

642 Rea, B.R., 2009. Defining modern day area-altitude balance ratios (AABRs) and their use in glacier-
643 climate reconstructions. *Quat. Sci. Rev.* *28*, 237–248.

644 Rea, B.R., Evans, D.J.A., 2007. Quantifying climate and glacier mass balance in north Norway during
645 the Younger Dryas. *Palaeogeogr. Palaeoclimatol. Palaeoecol.* *246*, 307-330.

646 Ribolini, A., 2000. Relief distribution, morphology and Cenozoic differential uplift in the Argentera
647 Massif (French–Italian Alps). *Z. Geomorphol.* *44*, 363–378.

648 Ribolini, A., Spagnolo, M., 2008. Drainage network geometry versus tectonics in the Argentera Massif
649 (French-Italian Alps). *Geomorphology* *93*, 253–266.

650 Schindelwig, I., Akçar, N., Kubik, P.W., Schlüchter, C., 2012. Lateglacial and early Holocene dynamics
651 of adjacent valley glaciers in the Western Swiss Alps. *J. Quaternary Sci.* *27*, 114-124.

652 Schönswetter, P., Stehlik, I., Holderegger, R., Tribsch, A., 2005. Molecular evidence for glacial refugia
653 of mountain plants in the European Alps. *Mol. Ecol.* *14*, 3547-3555.

654 Schorr, G., Pearman, P.B., Guisan, A., Kadereit, J.W., 2013. Combining palaeodistribution modelling
655 and phylogeographical approaches for identifying glacial refugia in Alpine *Primula*. *J Biogeogr* *40*,
656 1947–60.

657 Scotti, R., Brardinoni, F., Crosta, G.B., Cola, G., Mair, V., 2017. Time constraints for post-LGM landscape
658 response to deglaciation in Val Viola, Central Italian Alps. *Quat. Sci. Rev.*, *177*, 10-33.

659 Seguinot, J., Ivy-Ochs, S., Juvet, G., Huss, M., Funk, M., Preusser, F., 2018. Modelling last glacial cycle
660 ice dynamics in the Alps. *Cryosphere* *12*, 3265-3285.

- 661 Serrano, E., Gómez-Lende, M., González-Amuchastegui, M.J., González-García, M., González-Trueba,
662 J.J., Pellitero, R., Rico, I., 2015. Glacial chronology, environmental changes and implications for human
663 occupation during the upper Pleistocene in the eastern Cantabrian Mountains. *Quat. Int.* 364, 22-34
- 664 Shakun, J. D., Carlson, A.E., 2010. A global perspective on Last Glacial Maximum to Holocene climate
665 change. *Quat. Sci. Rev.* 29, 1801-1816.
- 666 Shilling, D.H., Hollin, J.T., 1981. Numerical reconstructions of valley glaciers and small icecaps. In:
667 Denton, G. H., Hughes, T. J. (Eds.), *The Last Great Ice Sheets*. Wiley, New York, 207–220.
- 668 Spotl, C., Mangini, A., 2007. Speleothems and glaciers. *Earth Planet. Sci. Lett.* 254, 323-331.
- 669 Stehlik, I., 2003. Resistance or emigration? Response of alpine plants to the ice ages. *Taxon* 52, 499-
670 510.
- 671 Tzortzis, S., Mocci, F., Walsh, K., Talon, B., Court-Picon, M., Dumas, V., Py Saragaglia, V., Richer, S.,
672 2008. Les massifs de l'Argentiérois du Mésolithique au début de l'Antiquité: au croisement des
673 données archéologiques et paléoenvironnementales en haute montagne (Hautes-Alpes, parc national
674 des Ecrins). *Le peuplement de l'arc alpin*. Paris, Éd. du CTHS, 2008, p. 123-148.
- 675 van der Bilt, W.G.M., Rea, B.R., Spagnolo, M., Roerdink, D.L., Jørgensen, S.L., Bakke, J., 2018. Novel
676 sedimentological fingerprints link shifting depositional processes to Holocene climate transitions in
677 East Greenland. *Glob. Planet. Chang.* 164, 52-64.
- 678 Weber, M.-J., Grimm, S.B., Baales, M., 2011. Between warm and cold: Impact of the Younger Dryas on
679 human behavior in Central Europe. *Quat. Int.* 242, 277-301.
- 680
681
682
683